DYNAMIC PERFORMANCE OF A BIO-INSPIRED UUV: EFFECTS OF FIN GAITS AND ORIENTATION

Jason D. Geder[1], Ravi Ramamurti[1], John Palmisano[2], Marius Pruessner[2], Banahalli Ratna[2], William C. Sandberg[3]

[1] Laboratory for Computational Physics and Fluid Dynamics,
Naval Research Laboratory, 4555 Overlook Ave., Washington, DC, 20375
[2] Center for Bio-molecular Science and Engineering,
Naval Research Laboratory, 4555 Overlook Ave., Washington, DC, 20375
[3] Modeling and Analysis Division,
Science Applications International Corporation, 1710 SAIC Dr., McLean, VA 22102

Abstract

The analysis of a proposed fin configuration change to a four-fin unmanned underwater vehicle (UUV) is described in this paper. Based on unsteady flow computations and experimental fin measurements, the forces and moments produced by the fins are evaluated for two fin configurations. As a result of this study, a change is made to a design that enables improved control symmetry in thrust production, higher reverse thrust and yaw moment production in hover, and higher forward thrust production at one knot forward speed. Vehicle responses to heading and depth commands are presented to validate improved vehicle performance.

This fin configuration change provides an added benefit of eliminating vehicle forward thrust when all four fins use the same gait – a set of rib and stroke motions. This allows us to propose and analyze a new lift producing fin gait which is also described in this paper. The new gait, combined with previously used lift producing fin motions, provides improved vehicle lift in hover. Open-loop vehicle depth response to two different lift gaits is compared to validate improved performance enabled by the new gait.

Introduction

Current operational unmanned underwater vehicles (UUVs) excel at many critical tasks including deeply submerged and high-endurance operations, performing high-speed and large-radius maneuvers. However, the traditional propeller-driven vehicles performing these missions have not demonstrated the same levels of operational success in cluttered, near-shore environments where precise positioning and small-radius maneuvers are required in the presence of waves and alternating currents. Researchers have therefore studied the fin force production mechanisms employed by various fish species in their attempts to understand how these organisms achieve high maneuverability and control authority in difficult environments [1][2]. Within fish swimming, articulation of the pectoral fins has been shown to produce forces and moments ideal for high-maneuverability in low-speed and hovering operations [3]. Several investigators have developed and adapted passively deforming robotic pectoral fins onto UUVs [4][5][6][7], whereas others have pursued the development of active control deformation pectoral fins [8][9][10].

To enable unmanned vehicle missions in near-shore underwater environments, we have studied the swimming mechanisms of a particular coral reef fish, the Bird wrasse (*Gomphosus varius*). Inspired by the pectoral fin of this species, we have designed a robotic fin based on computational fluid dynamics (CFD) and experimental studies of the forces and moments generated by the fin flapping motions. The resulting robotic fin uses active curvature control through actuation of individual ribs to produce desired propulsive forces (Figure 1).

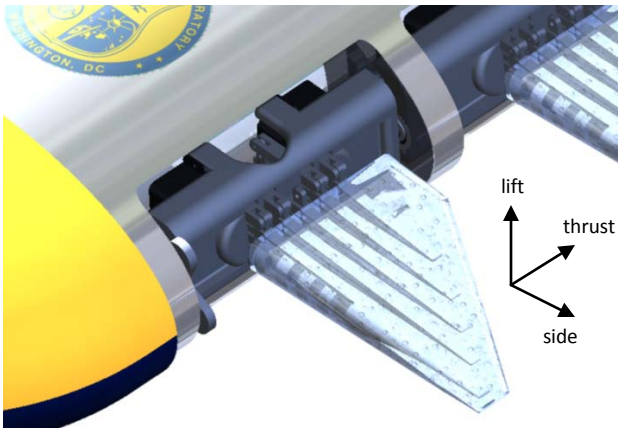

Fig. 1. Actively controlled curvature robotic pectoral fin mounted on custom designed UUV hull.

Our current work focuses on the integration of the robotic fin onto a UUV platform. After studying the performance of a two-fin vehicle [11][12], a four-fin vehicle configuration was designed and built to enable more precise control over the vehicle dynamics. Within the vehicle design, further CFD studies have helped identify fin-fin and fin-body interactions that are accounted for in vehicle models [13].

The scope of this paper is to analyze the vehicle configuration and fin kinematics with the goal of improving vehicle dynamic performance. First, we compare the maneuvering capabilities of the current vehicle configuration [14] with those enabled by a newly designed alternate configuration. While both configurations include four flapping fins, the orientation of these fins differ which impacts force generation and control authority. Second, we model vehicle lift generation and validate this model through experimental and computational results. We also introduce a new actively controlled fin stroke for improved lift generation over the current lift generating stroke.

Vehicle Fin Orientation

Initial fin configuration on the four-fin vehicle was designed to achieve maximum forward thrust capability based on computational and experimental results of an individual fin [9][15]. These results showed that a fin gait – a set of fin kinematics defined by rib deflections and fin stroke time-histories – can be designed to produce higher magnitude positive thrust than another gait can be designed to produce negative thrust, as defined in Figure 1. This positive thrust production propels the vehicle in the direction of the longer fin edge. Based on these studies, the original four-fin vehicle design incorporated all fins pointed in the same direction with the longer edge of the fin facing the front of the vehicle in a 'traditional' configuration (Figure 2a).

However, because of the asymmetry in forward and reverse thrust generation capability inherent in this 'traditional' fin configuration, control authority over vehicle yaw was low. Computational studies were carried out to determine how a 180° change in the orientation of the two rear fins on the vehicle – improving fore-aft vehicle symmetry – would affect force production capability [13] (Figure 2b). While it was expected this 'flipped' configuration would allow for improved turning and reverse motion performance, it also showed improvement in thrust generation at a one knot forward speed. The Because computational studies showed there was no apparent downside to this design change, the hardware configuration was amended to allow for an experimental validation.

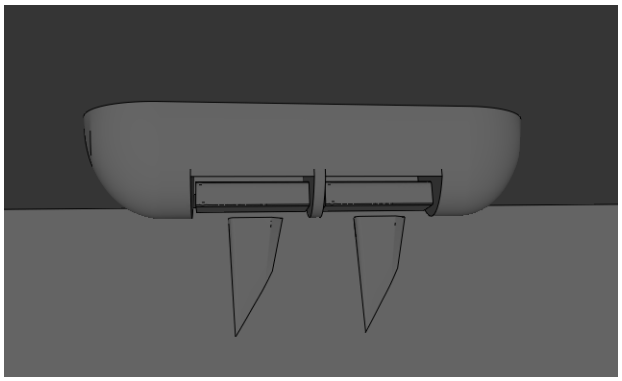

(a)

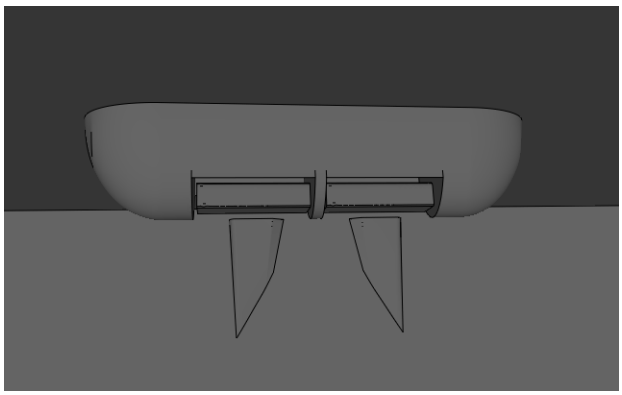

(b)

Fig. 2. Computer generated half-body models of the (a) 'traditional' and (b) 'flipped' fin configurations.

Based on the CFD studies of the fin configurations in Figure 2 [13], a comparison between the two designs is conducted in simulation and experiments. Vehicle models are first amended to create an accurate representation of the 'flipped' fin vehicle. While the rear fins in this configuration have the longer edge of the fin facing backwards, we still define fin thrust in the direction from longer edge to shorter edge as in Figure 1. In the equations for the vehicle, the effects of fin thrust and lift on vehicle dynamics are modified from Geder et al [14] to account for this orientation change (Equation 1).

$$\vec{\tau}_{fins} = \begin{bmatrix} f_{T,LF} - f_{T,LB} + f_{T,RF} - f_{T,RB} \\ 0 \\ -f_{L,LF} - f_{L,LB} - f_{L,RF} - f_{L,RB} \\ -y_L\left(f_{L,LF} + f_{L,LB}\right) - y_R\left(f_{L,RF} + f_{L,RB}\right) \\ x_F\left(f_{L,LF} + f_{L,RF}\right) + x_B\left(f_{L,LB} + f_{L,RB}\right) \\ -y_L\left(f_{T,LF} - f_{T,LB}\right) - y_R\left(f_{T,RF} - f_{T,RB}\right) \end{bmatrix} \quad (1)$$

Here, f_T is fin thrust, and f_L is fin lift. Subscripts 'LF', 'LB', 'RF', and 'RB' identify the left front, left back, right front, and right back fins, respectively. The x-position of the center of pressure on the fins is denoted by x_F for the front fins and x_B for the back fins. The y-position of the center of pressure on the fins is denoted by y_L for the left fins and y_R for the right fins. The center of pressure defines the location of the fin generated forces which is needed to compute the fin generated moments, and was determined using CFD as described by Palmisano et al [16].

With the 'traditional' orientation, and using the fin gaits currently programmed on the four-fin vehicle, the vehicle controller needs to account for asymmetries in force production of the 'forward' and 'reverse' gaits to hold position and perform yaw maneuvers [17]. Following Equation 1, and based on previous computations and experiments on fin force production [14][15], the 'flipped' configuration provides better force production symmetry on the vehicle leading to increased control authority over positioning.

The -0.60 N of thrust generated by the 'flipped' configuration (with two front fins using 'reverse' gait and two back fins using 'forward' gait) at zero free stream flow is a 58% improvement in thrust magnitude over the -0.38 N generated by the 'traditional' configuration (with all four fins using 'reverse' gait). This improves stopping and backing up, and is important in maintaining position in the presence of external flows. Also, while the maximum yaw moment generated by the two configurations is equal (0.061 N·m), this moment is only achievable in hover by the 'flipped' configuration. Attaining the maximum yaw moment with the 'traditional' configuration would also generate forward thrust as the 'forward' kinematics of the pair of fins on one side of the vehicle would produce larger magnitude thrust than the 'reverse' kinematics on the other side of the vehicle. The largest yaw moment in hover that the 'traditional' configuration allows is 0.039 N·m, indicating a 56% improvement for the 'flipped' configuration.

Simulation of vehicle models and experiments on the two different configurations validate that the desired force and control symmetry is achieved with the 'flipped' fin configuration. Experimental results of vehicle yaw motion in hover, shown in Figure 3, demonstrate that the 'flipped' configuration yields a maximum yaw rate of 41 °/s, a 24% improvement in yaw rate over the 33 °/s allowed by the 'traditional' configuration. The results also validate the vehicle model in yaw as all experimental data points fall within 10° of simulation results.

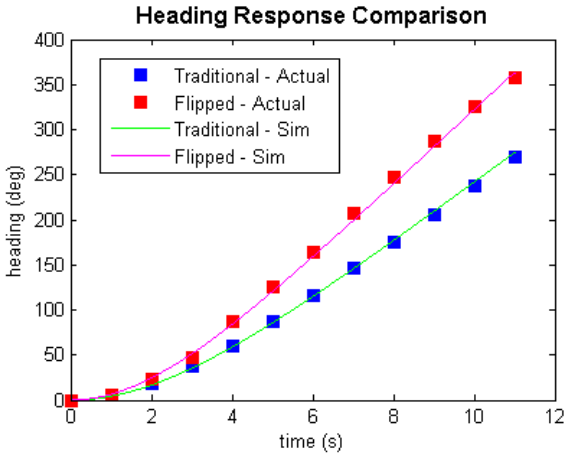

Fig. 3. Simulated and experimental vehicle yaw responses in hover to maximum allowable fin generated yaw moments for the 'traditional' and 'flipped' in configurations.

Vehicle Performance

Using the previously presented vehicle controller [14], the response to combined depth and heading commands for the 'flipped' configuration vehicle has been measured in simulation and experiments, and the results are shown in Figure 4.

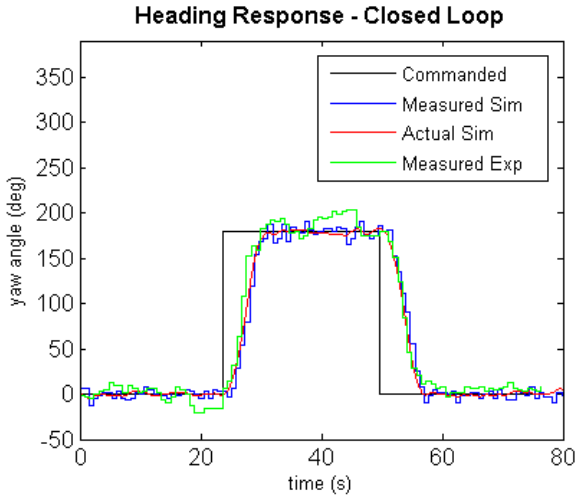

(a)

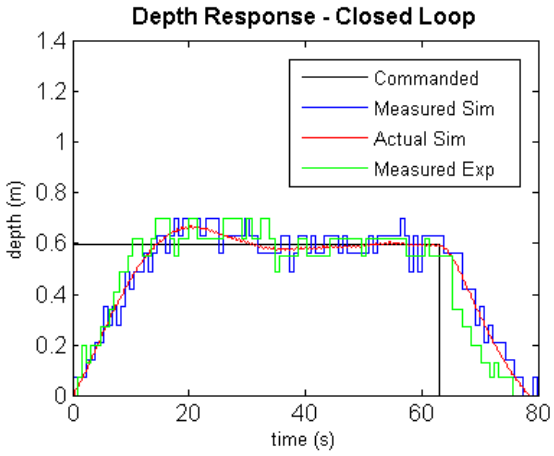

(b)

Fig. 4. Simulated and experimental closed-loop vehicle responses to (a) commanded heading and (b) commanded depth.

With a critically damped rise time of ~5s to reach the commanded 180° heading angle change, we see improvement over the ~7s rise time for the 'traditional' configuration previously presented [14]. Depth response remains unchanged, as control over lift is decoupled from control over thrust for low speeds [11]. These results demonstrate how, with no change to the fin gaits or controller, an improvement in vehicle yaw response is accomplished by changing fin orientation.

Vehicle Lift Production

In addition to the benefits on thrust and yaw moment allowed by the 'flipped' fin configuration, the symmetry introduced by this design makes decoupling vehicle lift from thrust in hover easier as well. Equation 1 shows vehicle thrust and vehicle yaw moment will be zero when the front and back fin kinematics are the same because they are producing equal and opposite fin thrust forces. In this special case, only fin generated lift will affect the vehicle, as shown in Equation 2.

$$f_{T,LF} = f_{T,LB} = f_{T,RF} = f_{T,RB},$$

$$\vec{\tau}_{fins} = \begin{bmatrix} 0 \\ 0 \\ -f_{L,LF} - f_{L,LB} - f_{L,RF} - f_{L,RB} \\ -y_L\left(f_{L,LF} + f_{L,LB}\right) - y_R\left(f_{L,RF} + f_{L,RB}\right) \\ x_F\left(f_{L,LF} + f_{L,RF}\right) + x_B\left(f_{L,LB} + f_{L,RB}\right) \\ 0 \end{bmatrix} \quad (2)$$

Because fin generated thrust has no effect on vehicle motion when all four fins are using the same fin kinematics allows for a simpler analysis of vehicle depth control in hover. This mode of motion is essential for the low-speed maneuvers desired of this vehicle, and analysis of lift producing fin kinematics at these zero forward speed conditions are presented in the following section.

Methods for producing lift forces by the pectoral fins have been studied both computationally and experimentally [9][11][15]. A lift producing fin gait was designed and named 'lift gait'. This 'lift gait' holds the fin flat and rigid during the downstroke to produce upward lift, and then spreads the ribs apart on the upstroke with rib 1 leading the upstroke and rib 5 trailing to reduce downward lift (Figure 5a). Subsequent work on a two-fin vehicle highlighted the benefits of a different means of lift production in which the mean fin stroke angle is biased up or down to produce lift [11].

To investigate other potentially improved lift producing fin kinematics, a third fin gait called the 'cupped gait' is designed to produce lift, and the actual kinematics of the rib motions are measured. This gait has a 'cupped' shape where the leading and trailing edge ribs (ribs 1 and 2) are deflected in the same direction, while the middle ribs are deflected in the opposite direction creating a cup shape when viewed in the spanwise direction (Figure 5b).

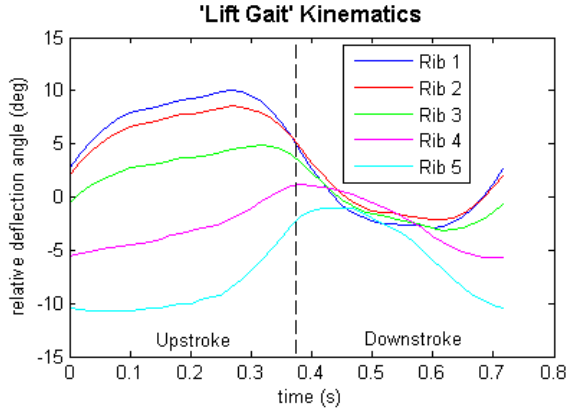

Fig. 5. Comparison of fin rib deflections for the (a) 'lift' gait and (b) 'cupped' gait throughout a 1.4 Hz frequency stroke.

A comparison of the forces produced by the 'lift gait', the 'cupped gait', and a 'rigid gait' – defined by zero relative rib deflection for all the ribs throughout the stroke – is presented in Figure 6. This comparison is made at zero freestream flow, and at a specified flapping frequency of 1.4 Hz, stroke amplitude of 78°, and stroke angle bias of 0°. As expected, the 'rigid gait' produces a near zero mean lift force (0.0004 N) as it has a symmetric stroke up and down. However, it does produce a side force of -0.0604 N, similar to how a caudal fin on a fish produces thrust. The 'lift gait' at these operating parameters also yields a near zero lift force (-0.0004 N) which is validated by experimental studies showing that lift force is not guaranteed using this gait, and depends highly on the frequency and amplitude of the stroke (Figure 7). Again, some side force is produced (-.0483 N) a slightly smaller value that may be attributed to the curvature changes of the fin. Finally, the 'cupped gait' produces a mean positive lift (0.0623 N), while also producing a side force similar to the 'rigid gait' (-0.0690 N).

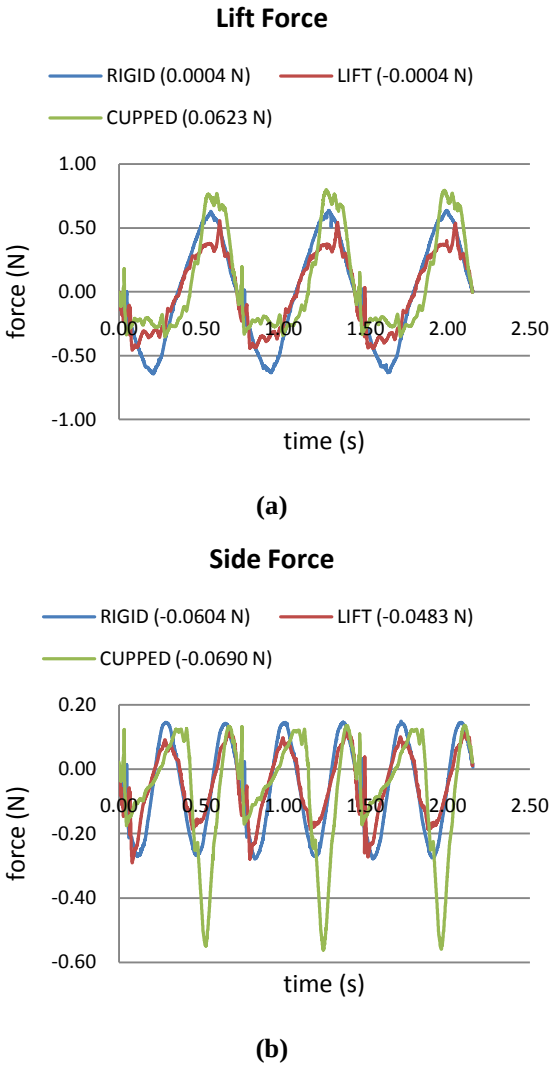

Fig. 6. Comparison of fin generated (a) lift and (b) side forces for the 'rigid', 'lift', and 'cupped' gaits throughout a 1.4 Hz frequency and 78° amplitude stroke.

While the 'lift gait' did not produce any mean lift for the specific stroke frequency and amplitude presented in Figure 6, there are operating conditions where this gait has produced lift experimentally. However, we can see from the experimental results that the lift produced by this gait is not very consistent or predictable across a range of stroke amplitudes and frequencies (Figure 7). High lift is seen at both higher frequencies (4-5 Hz) and lower frequencies (~1 Hz) for certain stroke amplitudes, but there are very quick drops to low lift production. In a vehicle mission scenario where robustness to changing parameters is needed, these rapid changes would render this method of lift control unusable.

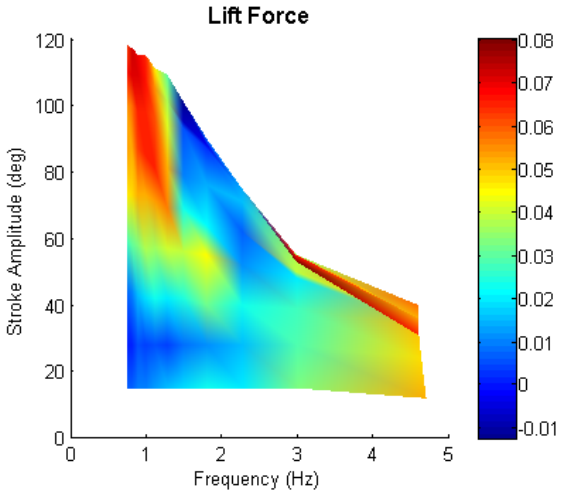

Fig. 7. Experimental lift from the 'lift' gait as a function of stroke frequency and amplitude.

Currently, the four-fin vehicle employs the use of biasing the mean stroke angle of the fins to produce lift (Figure 8). Equation 3 defines the effect of fin bias on vehicle lift, showing how fin side force contributes. Combinations of a 'forward gait' and a 'reverse gait' are used to produce thrust. These gaits differ only in the relative deflections of each of the ribs which are equal in magnitude to and opposite in direction from each other. This means that when 50% 'forward gait' and 50% 'reverse gait' are used, a 'rigid gait' is produced.

$$f_{L,\,vehicle} = f_{L,\,fin}\cos(\Phi_{bias}) - f_{S,\,fin}\sin(\Phi_{bias}) \qquad (3)$$

Here $f_{L,vehicle}$ is the force generated by a single fin in the vehicle lift direction, $f_{L,fin}$ is the force in the fin lift direction, $f_{S,fin}$ is the force in the fin side direction, and Φ_{bias} is the bias of the stroke angle above horizontal.

Based on the limited fin force results presented in Figure 6, a combination of the 'cupped gait' with mean fin stroke angle bias will improve on the lift production we are currently getting with biasing of the 'forward gait' and 'reverse gait'. Initial results suggest that combining these two methods using the new fin gait yields a 190% increase in vehicle lift generation enabling increased control authority over heave, pitch, and roll (Figure 9).

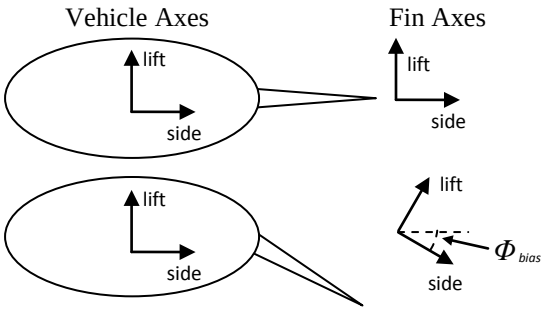

Fig. 8. Diagram of lift and side forces in the vehicle and fin axes.

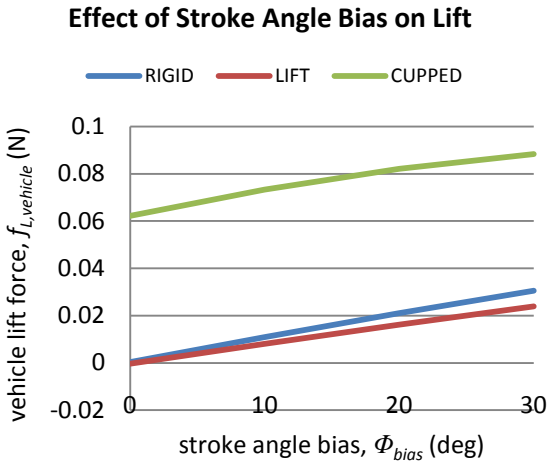

Fig. 9. Computed fin lift as a function of stroke angle bias for the 'rigid', 'lift', and 'cupped' gaits throughout a 1.4 Hz frequency and 78° amplitude stroke.

Vehicle Performance

Vehicle performance in depth has been measured experimentally using mean stroke angle bias to produce lift, but with combinations of the 'forward gait' and 'reverse gait' defining the individual rib motions (Figure 10a). These experiments have validated our computational

models of the vehicle, and we can therefore use the computations of the 'cupped gait' to compare vehicle performance in vertical motion. As expected, because the biased 'cupped gait' produces three times greater lift force on the vehicle, the maximum vertical velocity is ~1.7 times greater as shown in Figure 10b (0.112 m/s for biased 'cupped', 0.065 m/s for biased 'rigid'), as $F \propto V^2$.

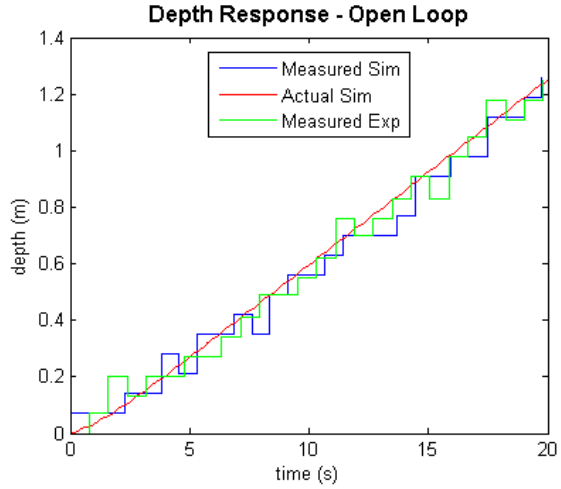

(a)

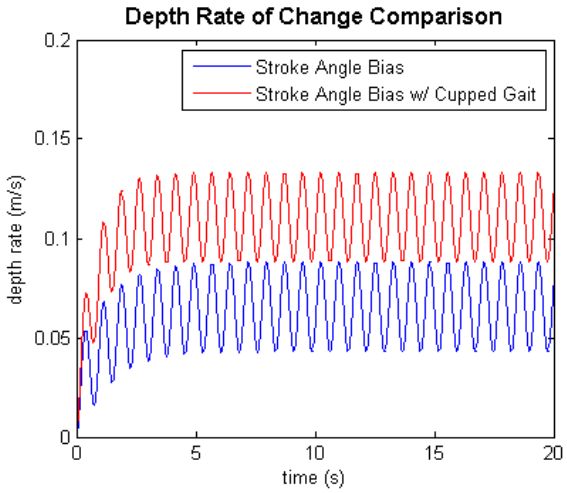

(b)

Fig. 10. (a) Simulated and experimental vehicle depth responses to all four fins using the 'rigid' gait with 30° fin stroke angle bias. (b) Comparison of simulated depth rate responses for 'rigid' and 'cupped' gaits with 30° fin stroke angle bias.

In addition to the benefits the 'cupped' gait provides, there are also downsides. While the 'flipped' configuration of the fins eliminates any total thrust generated by the vehicle in hover, a combination of a thrust producing gait and lift producing gait is for depth change while translating forward or backward. Using the 'cupped' gait as the lift producing gait, the combination with 'forward' or 'reverse' gait does not produce a curvature that is necessarily ideal. Just biasing the fins to produce lift effectively decouples thrust and lift control in hover and in translation [11][14], which makes it an appealing choice. The lift benefits of the 'cupped' gait cannot be ignored, however, and in future experiments we propose using the cupped gait in applications where zero horizontal translation is desired as we move up and down and vertical column. In translational maneuvers, the 'cupped' gait will be eliminated to facilitate decoupled control over thrust and lift.

Conclusions

We have determined that a change in fin orientation for a four-fin bio-inspired UUV, which introduces better fore-aft symmetry to the vehicle, increases control authority by enabling improvement in fin force generation. In horizontal plane motion, the new 'flipped' orientation produces more than 58% higher reverse thrust and 56% higher yaw moment in the vehicle at low speeds, and higher forward thrust at higher vehicle speeds. In vertical motion, the symmetry introduced by the 'flipped' orientation enables a new fin gait called the 'cupped' gait which, in combination with fin stroke angle biasing, produces nearly three times (2.9 times) the vehicle lift force of previous methods. Vehicle simulations and experiments validate the fin force production results, showing that the new fin orientation and new lift producing fin gait add performance benefits in horizontal and vertical translation, as well as in yaw rotation. Overall, the new vehicle configuration increases the vehicle maneuverability envelope, improving potential mission performance.

References

1. J. E. Colgate and K. M. Lynch, "Mechanics and Control of Swimming: A Review," *IEEE Journal of Oceanic Engineering*, vol. 29, pp. 660-673, 2004.
2. P. R. Bandyopadhyay, "Trends in biorobotic autonomous undersea vehicles," *IEEE Journal of Oceanic Engineering*, vol. 30, pp. 109-139, 2005.

3. R. W. Blake, “The mechanics of labriform motion I. Labriform locomotion in the angelfish (*pterophyllum eimekei*): An analysis of the power stroke”, J*ournal of Experimental Biology*, vol. 82, 1979, pp. 255-271.
4. N. Kato, “Hydrodynamic Characteristics of a Mechanical Pectoral Fin”, *Journal of Fluids Engineering, Transactions of the ASME*, vol. 121, pp. 605-613, 1999.
5. N. Kato, “Control Performance of a Fish Robot with Mechanical Pectoral Fins in the Horizontal Plane”, *Journal of Oceanic Engineering, Transactions of the IEEE*, vol. 25, no. 1, 2000.
6. B. Hobson, M. Murray, and C. A. Pell, “PilotFish: Maximizing Agility in an Unmanned-Underwater Vehicle”, *Proceedings of the International Symposium on Unmanned Untethered Submersible Technology*, Durham, NH, 1999.
7. S. Licht, V. Polidoro, M. Flores, F. S. Hover, and M. S. Triantafyllou, “Design and Projected Performance of a Flapping Foil AUV”, *IEEE Journal of Oceanic Engineering*, vol. 29, no. 3, 2004.
8. Y. Ando, N. Kato, H. Suzuki, T. Ariyoshi, K. Suzumori, T. Kanda, and S. Endo, “Elastic Pectoral Fin Actuators for Biomimetic Underwater Vehicles”, *Proceedings of the 16th International Offshore and Polar Engineering* Conference, pp. 260-267, 2006.
9. J. Palmisano, R. Ramamurti, K.J. Lu, J. Cohen, W. C. Sandberg, and B. Ratna, “Design of a Biomimetic Controlled-Curvature Robotic Pectoral Fin”, *2007 IEEE Int. Conf. on Robotics and Automation*, Rome, Italy.
10. K. W. Moored, W. Smith, W. Chang, and H. Bart-Smith, “Investigating the thrust production of a myliobatoid-inspired oscillating wing”, *3rd International CIMTEC Conference*, Acireale, Italy, June 8-13, 2008.
11. J. D. Geder, J. Palmisano, R. Ramamurti, W. C. Sandberg, and B. Ratna, “Fuzzy Logic PID Based Control Design and Performance for Pectoral Fin Propelled Unmanned Underwater Vehicle”, *International Conference on Control, Automation, and Systems*, Seoul, Korea, October 14-17, 2008.
12. J. D. Geder, R. Ramamurti, J. Palmisano, M. Pruessner, B. Ratna, and W. C. Sandberg, “Sensor Data Fusion and Submerged Test Results of a Pectoral Fin Propelled UUV”, *16th International Symposium on Unmanned Untethered Submersible Technology*, Durham, New Hampshire, USA, August 23-26, 2009.
13. R. Ramamurti, J. Geder, J. Palmisano, M. Pruessner, B. Ratna, and W. Sandberg, “3-D Unsteady Computational Studies of a Four-Fin Bio-Inspired UUV”, submitted to *17th International Symposium on Unmanned Untethered Submersible Technology*, Portsmouth, New Hampshire, USA, August 21-24, 2011.
14. J. D. Geder, R. Ramamurti, J. Palmisano, M. Pruessner, W. C. Sandberg, B. Ratna, “Four-fin Bio-inspired UUV: Modeling and Control Solutions”, *ASME International Mechanical Engineering Congress and Exposition*, IMECE 2011-64005, 2011.
15. R. Ramamurti, J. D. Geder, J. Palmisano, B. Ratna, and W. C. Sandberg, “Computations of Flapping Flow Propulsion for Unmanned Underwater Vehicle Design”, *AIAA Journal*, Vol. 48, No. 1, pp. 188-201, January 2010.
16. J. S. Palmisano, J. D. Geder, R. Ramamurti, M. Pruessner, W. C. Sandberg, and B. Ratna, “Robotic Pectoral Fin Thrust Vectoring Using Weighted Gait Combinations”, submitted for publication in *Applied Bionics and Biomechanics*, November 2010.